Dispersion characteristics of two-dimensional unmagnetized dielectric plasma photonic crystal*

Qi Li-Mei(亓丽梅)[a)†], Yang Zi-Qiang(杨梓强)[a)], Lan Feng(兰 峰)[a)], Gao Xi(高 喜)[a)], and Li Da-Zhi(李大治)[b)]

[a)] *Institute of High Energy Electronics, University of Electronic Science and Technology of China, Chengdu* 610054, *China*
[b)] *Institute for Laser Technology*, 2-6 *Yamada-Oka, suita, Osaka* 565-0871, *Japan*

(Received 9 March 2009; revised manuscript received 8 June 2009)

This paper studies dispersion characteristics of the transverse magnetic (TM) mode for two-dimensional unmagnetized dielectric plasma photonic crystal by a modified plane wave method. First, the cutoff behaviour is made clear by using the Maxwell–Garnett effective medium theory, and the influences of dielectric filling factor and dielectric constant on effective plasma frequency are analysed. Moreover, the occurence of large gaps in dielectric plasma photonic crystal is demonstrated by comparing the skin depth with the lattice constant, and the influence of plasma frequency on the first three gaps is also studied. Finally, by using the particle-in-cell simulation method, a transmission curve in the $\Gamma - X$ direction is obtained in dielectric plasma photonic crystal, which is in accordance with the dispersion curves calculated by the modified plane wave method, and the large gap between the transmission points of 27 GHz and 47 GHz is explained by comparing the electric field patterns in particle-in-cell simulation.

Keywords: plasma photonic crystal, dispersion, plane wave method, particle-in-cell simulation
PACC: 4270Q, 5240H

1. Introduction

Photonic crystal (PC) has attracted much attention since the initial predictions of Yablonovitch[1] and John.[2] This active research area has been extended to plasma PCs which is expected to obtain many new particular characteristics,[3−11] various diagnostics revealed that electron plasma density $n_{\rm e} = 10^{12} - 10^{16}$ cm^{-3}, which corresponds to electron plasma frequency $\omega_{\rm p}/2\pi = 10 - 1000$ GHz, that means plasma PC can dynamically control electromagnetic waves from microwaves to THz waves.[7,8] Recently, the experiments of millimeter waves propagating through two-dimensional (2D) unmagnetized plasma PCs demonstrated that the existence of a unidirectional photonic band gap is stable, and the experimental results were consistent with the dispersion curves calculated theoretically.[8−10] Most of the works mentioned above focused on 2D plasma PC composed of vacuum and plasma, the aim of this present study is to investigate the 2D dielectric plasma PC (DPPC) in which dielectric rods are arranged in plasma, only dispersion characteristic of the transverse magnetic (TM) mode is considered here since there are cutoff behaviour and large omnidirectional band gaps compared with the transverse electric (TE) mode. To explain the cutoff behaviour, the Maxwell–Garnett effective medium theory is used in this paper and the theoretical analysis is consistent with the numerical result, and effective plasma frequency as a function of dielectric filling factor and dielectric constant are given. By comparing with the skin depth with the lattice constant, the occurence of large omnidirectional gaps is demonstrated, the first three gaps versus plasma frequency are analysed. Finally, 2D particle-in-cell (PIC) simulation is carried out to investigate the features of wave propagation in DPPC.

2. Theoretical model and modified plane wave method

Figure 1 shows the schematic structure of 2D square lattice DPPC in which dielectric rods are periodically arranged in the $x - y$ plane of plasma. We assume that the length of square rods and lattice constant are L and a respectively, relative dielectric functions of the square rods and background are $\varepsilon_{\rm a}$ and $\varepsilon_{\rm b}$ respectively.

*Project supported by the National Natural Science Foundation of China (Grant Nos. 60571020 and 10975031)
†Corresponding author. E-mail: qilimei1204@163.com
© 2010 Chinese Physical Society and IOP Publishing Ltd

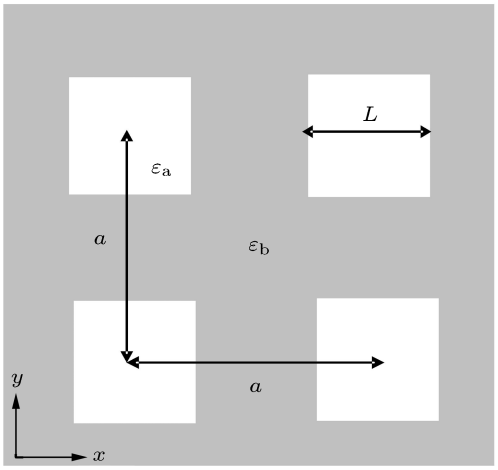


Fig. 1. Schematic structure of 2D square lattice DPPC.

For the collisionless unmagnetized plasma in the background, we utilize the frequency-dependent dielectric function ε_b that meets the Drude formula:[3]

$$\varepsilon_b(\omega) = 1 - \frac{\omega_p^2}{\omega^2}, \tag{1}$$

where ω is electromagnetic wave frequency, electron plasma frequency $\omega_p = (e^2 n_e/\varepsilon_0 m)^{1/2}$ in which e, m and ε_0 are electric quantity, electric quality and dielectric constant in vacuum.

Many theoretical and numerical tools have been developed to calculate the dispersion curves of PCs, such as the plane wave method (PWM),[12−14] finite-difference time-domain (FDTD) method,[4,15] transfer-matrix method[16] and multiple scattering method.[17,18] Among these methods, PWM is the more popular technique. In this paper, we will modify the PWM eigenequation to a standard one that is capable of analysing the DPPC structure.

The eigenvalue equation of the TM mode where electric vector of field is parallel to rods can be written as[13]

$$\begin{aligned}\left|\boldsymbol{k}_\parallel + \boldsymbol{G}_\parallel\right|^2 B(\boldsymbol{k}_\parallel, \boldsymbol{G}_\parallel) &= \frac{\omega^2}{c^2}\sum_{\boldsymbol{G}'_\parallel} \hat{\varepsilon}(\boldsymbol{G}_\parallel - \boldsymbol{G}'_\parallel) B(\boldsymbol{k}_\parallel, \boldsymbol{G}'_\parallel) \\ &= \frac{\omega^2}{c^2}\hat{\varepsilon}(0) B(\boldsymbol{k}_\parallel, \boldsymbol{G}_\parallel) + \frac{\omega^2}{c^2}\sum_{\boldsymbol{G}'_\parallel \neq \boldsymbol{G}_\parallel} \hat{\varepsilon}(\boldsymbol{G}_\parallel - \boldsymbol{G}'_\parallel) B(\boldsymbol{k}_\parallel, \boldsymbol{G}'_\parallel),\end{aligned} \tag{2}$$

where c is the speed of light in vacuum, $\boldsymbol{k}_\parallel$ is wave vector, and $\boldsymbol{G}_\parallel = G_x\boldsymbol{x} + G_y\boldsymbol{y}$ is the reciprocal vector, $B(\boldsymbol{k}_\parallel, \boldsymbol{G}_\parallel)$ and $\widehat{\varepsilon}(\boldsymbol{G}_\parallel)$ are the Fourier coefficients of electric field E_z $(\boldsymbol{k}_\parallel, \boldsymbol{r}_\parallel)$ and position-dependent dielectric function $\varepsilon(\boldsymbol{r}_\parallel)$, respectively.

The Fourier coefficient $\widehat{\varepsilon}(\boldsymbol{G}_\parallel)$ for position-dependent dielectric function $\varepsilon(\boldsymbol{r}_\parallel)$ in Fig. 1 can be written as

$$\widehat{\varepsilon}(\boldsymbol{G}_\parallel) = \begin{cases} \left(1 - \dfrac{\omega_p^2}{\omega^2}\right) + \left(\varepsilon_a - 1 + \dfrac{\omega_p^2}{\omega^2}\right) f, & \boldsymbol{G}_\parallel = 0, \\ \left(\varepsilon_a - 1 + \dfrac{\omega_p^2}{\omega^2}\right) P(\boldsymbol{G}_\parallel), & \boldsymbol{G}_\parallel \neq 0, \end{cases} \tag{3}$$

where $P(\boldsymbol{G}_\parallel) = f\dfrac{\sin(G_x L/2)}{G_x L/2}\dfrac{\sin(G_y L/2)}{G_y L/2}$ and $f = \dfrac{L^2}{a^2}$ is the filling factor in one unit cell.

Substituting Eq. (3) into Eq. (2) and making the transformation, we get the eigenvalue equation of the TM mode for the DPPC,

$$\begin{aligned}&\sum_{\boldsymbol{G}'_\parallel}\left\{\left|\boldsymbol{k}_\parallel + \boldsymbol{G}_\parallel\right|^2 \delta_{\boldsymbol{G}_\parallel, \boldsymbol{G}'_\parallel} + \frac{\omega_p^2}{c^2}[\delta_{\boldsymbol{G}_\parallel, \boldsymbol{G}'_\parallel} - P(\boldsymbol{G}_\parallel - \boldsymbol{G}'_\parallel)]\right\} B(\boldsymbol{k}_\parallel, \boldsymbol{G}'_\parallel) \\ &= \frac{\omega^2}{c^2}\sum_{\boldsymbol{G}'_\parallel}[\delta_{\boldsymbol{G}_\parallel, \boldsymbol{G}'_\parallel} + (\varepsilon_a - 1)P(\boldsymbol{G}_\parallel - \boldsymbol{G}'_\parallel)] B(\boldsymbol{k}_\parallel, \boldsymbol{G}'_\parallel).\end{aligned} \tag{4}$$

Equation (4) can be written as a standard eigenvalue equation

$$\left[(\boldsymbol{I} + \boldsymbol{V})^{-1}\boldsymbol{U} - \frac{\omega^2}{c^2}\right]\boldsymbol{B} = 0. \tag{5}$$

The elements of square matrices $\boldsymbol{U}, \boldsymbol{V}$ and $\boldsymbol{I}$ are defined as

$$\begin{aligned}\boldsymbol{U}(\boldsymbol{G}_\parallel|\boldsymbol{G}'_\parallel) &= \left|\boldsymbol{k}_\parallel + \boldsymbol{G}_\parallel\right|^2 \delta_{\boldsymbol{G}_\parallel,\boldsymbol{G}'_\parallel} \\ &\quad + \frac{\omega_{\rm p}^2}{c^2}[\delta_{\boldsymbol{G}_\parallel,\boldsymbol{G}'_\parallel} - P(\boldsymbol{G}_\parallel - \boldsymbol{G}'_\parallel)], \\ \boldsymbol{V}(\boldsymbol{G}_\parallel|\boldsymbol{G}'_\parallel) &= (\varepsilon_{\rm a} - 1)P(\boldsymbol{G}_\parallel - \boldsymbol{G}'_\parallel), \\ \boldsymbol{I}(\boldsymbol{G}_\parallel|\boldsymbol{G}'_\parallel) &= \delta_{\boldsymbol{G}_\parallel,\boldsymbol{G}'_\parallel}. \end{aligned} \tag{6}$$

Therefore, dispersion characteristics of the TM mode can be achieved by solving the standard eigenvalue problem for a real, symmetric matrix. On the other hand, the electric field can also be obtained from the eigenvectors of Eq. (5).

3. Results and discussion

3.1. Dispersion curves of DPPC

Figure 2 shows dispersion curves of the TM mode with normalized plasma frequency $\omega_{\rm p}a/2\pi c = 1$, relative dielectric constant of rods $\varepsilon_{\rm a} = 6$ and dielectric filling factor $f = 0.5$ respectively. The vertical axis denotes the normalized frequency $\omega a/2\pi c$, and the horizontal axis shows wave vector k varying along $\Gamma - X - M - \Gamma$. The insetted triangle indicates the first irreducible Brillouin zone defined in usually crystal theory, and points Γ, X, M are wave vector $\boldsymbol{k} = [0, 0]$, $[\pi/a, 0]$ and $[\pi/a, \pi/a]$ respectively. Gray areas represent omnidirectional band gaps where electromagnetic waves of the TM mode cannot propagate in any direction, and line curves together with circle points show pass bands. In the numerical calculation, two methods are used, the line curves are calculated by modified PWM based on Eq. (5), a total number of 441 plane waves are used. The circle points are obtained by frequency-dependent FDTD method[15] using a spatial grid resolution 40×40 points per lattice constant. Their results are in good agreement and indicate that our implementation of modified PWM is correct.

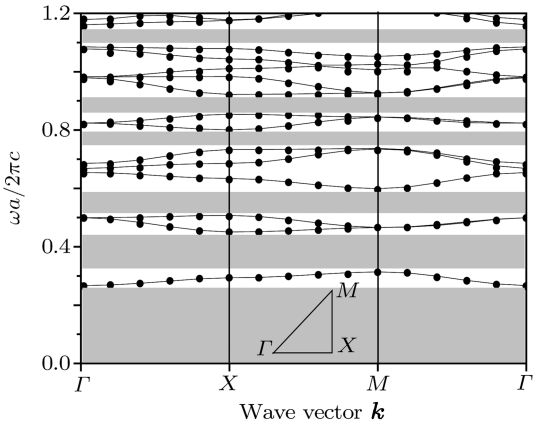


Fig. 2. Dispersion curves of the TM mode with $f = 0.5$, $\varepsilon_{\rm a} = 6$ and $\omega_{\rm p}a/2\pi c = 1$, insertted triangle indicates the first irreducible Brillouin zone, gray areas represent band gaps, line curves together with circle points show pass bands.

In Fig. 2, the first pass band starts from a normalized cutoff frequency $\Omega_{\rm p}a/2\pi c = 0.27$, where $\Omega_{\rm p}$ is the lowest cutoff frequency or effective plasma frequency (EPF),[19,20] while for a bulk plasma with $\omega_{\rm p}a/2\pi c = 1$, electromagnetic waves are evanescent and there is no eigenmode for $\omega_{\rm p}a/2\pi c < 1$. In the following we can apply the Maxwell–Garnett effective medium theory to explain this unique characteristic of DPPC.[21−23] If wavelength is long, eigenmodes are not affected by the detail of the spatial variation of dielectric function in the DPPC, the effective dielectric function of the DPPC can be given by the following relation:[22,23]

$$\frac{\varepsilon_{\rm eff}(\omega) - \varepsilon_{\rm b}(\omega)}{\varepsilon_{\rm eff}(\omega) + 2\varepsilon_{\rm b}(\omega)} = f\frac{\varepsilon_{\rm a}(\omega) - \varepsilon_{\rm b}(\omega)}{\varepsilon_{\rm a}(\omega) + 2\varepsilon_{\rm b}(\omega)}. \tag{7}$$

In this approximation, using the dispersion relation $k = \dfrac{\omega}{c}\sqrt{\varepsilon_{\rm eff}(\omega)}$, we can obtain the EPF $\Omega_{\rm p}$ as

$$\Omega_{\rm p} = \omega_{\rm p}\sqrt{\frac{(1-f)}{1 + \dfrac{\varepsilon_{\rm a}}{2} + (\varepsilon_{\rm a} - 1)f}}. \tag{8}$$

In Eq. (8), it is obvious that $\Omega_{\rm p}$ of the DPPC is lower than $\omega_{\rm p}$. Taking parameters in Fig. 2 into Eq. (8), we obtain $\Omega_{\rm p}a/2\pi c = 0.277$, which is very close to the value of 0.27 calculated by modified PWM.

In Fig. 3, circle (•) shows the normalized EPF versus dielectric filling factor f of the DPPC with $\varepsilon_{\rm a} = 6$ and $\omega_{\rm p}a/2\pi c = 1$. Solid line shows its nonlinear relationship by exponential decay function $\Omega_{\rm p}a/2\pi c = 0.089 + 0.447{\rm e}^{-f/0.537}$. Square (■) and triangle (▲) denote the normalized EPF versus f for different dielectric constants of rods $\varepsilon_{\rm a} = 8$ and $\varepsilon_{\rm a} = 3$ respectively, it is seen that they have similar trend as that of $\varepsilon_{\rm a} = 6$. However, for a given filling factor, the normalized EPF decreases as $\varepsilon_{\rm a}$ increases. Therefore, by choosing the dielectric constant and dielectric filling factor in DPPC, one can easily make the position of the normalized EPF to a target value.

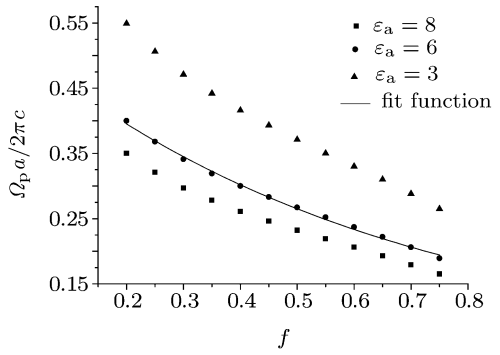


Fig. 3. Dependence of normalized EPF on dielectric filling factor f and dielectric constant ε_a with $\omega_p a/2\pi c = 1$. Triangle (▲), circle (●) and square (■) are the normalized EPFs for different dielectric constant $\varepsilon_a = 3$, 6 and 8 respectively. The solid line shows the nonlinear relationship of circle (●).

As can be seen from the gray areas in Fig. 2, besides the largest band gap between the zero frequency and EPF (named TM01), there are another five large omnidirectional band gaps which lie between the first and second pass bands (TM12), the third and fourth pass bands (TM34), the sixth and seventh pass bands (TM67), the eighth and ninth pass bands (TM89) and the thirteenth and fourteenth pass bands (TM1314) respectively. Reason of this feature becomes obvious if we compare the skin depth $\delta = c/\omega_p$[24] with the distance between the dielectric rods in plasma. Since the parameter δ/a is 0.16 in Fig. 2, which is much less than one, the coupling between the neighbouring dielectric rods is weak. This explains large gaps.

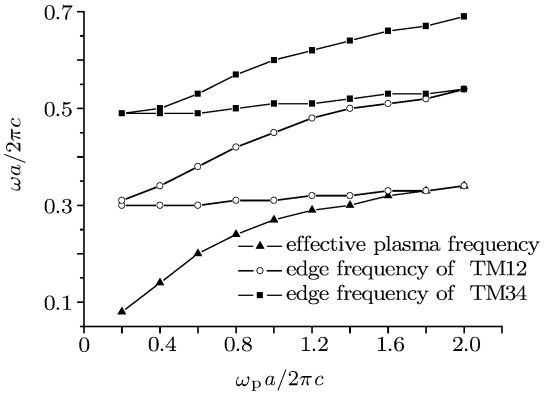


Fig. 4. Dependence of EPF, edge frequencies of the TM12 and TM34 on plasma frequency with $f = 0.5$ and $\varepsilon_a = 6$.

Furthermore, the coupling will become weaker as plasma frequency increases. To verify the influence of plasma frequency on band gaps in detail, Fig. 4 shows EPF, edge frequencies of the TM12 and TM34 as a function of normalized plasma frequency. It is seen that the EPF, edge frequencies of the TM12 and TM34 increase when normalized plasma frequency varies from 0.2 to 2. Simultaneously, distance between the EPF and the lower edge frequency of TM12 and that between the upper edge frequency of TM12 and the lower edge frequency of TM34 decrease. As a result, pass bands become narrow and gaps of TM01, TM12 and TM34 enlarge. Therefore, DPPC can be used as a dynamic electromagnetic wave controller by changing the plasma frequency.

3.2. Wave field pattern in PIC simulation

To obtain the propagation process of electromagnetic wave in DPPC, a PIC code named CHIPIC is used.[1)] The DPPC geometry in PIC simulation is shown in Fig. 5. There are 3×3 square lattice dielectric rods arranged in plasma background with lattice constant $a = 3$ mm and rod length $L = 2.12$ mm, then the filling factor f is equal to 0.5. Periodic boundary conditions are applied at the top and bottom of the geometry in the y direction. In the x direction, absorbing conditions are used with 0.5 mm thick. The source line shown with a straight line is close to the left absorbing boundary, and the incident source is set to realize the TM mode propagation in which electric field is parallel to the z plane. The detector line not shown in this model is parallel to the source line with a distance of 8.8 mm between them. The plasma is defined as a collisionless and uniform one with plasma density $n_e = n_i = 12.42 \times 10^{13}$ cm^{-3} in PIC simulation. Mesh sizes in the x and y direction are same with $dx = dy = 0.05$ mm.

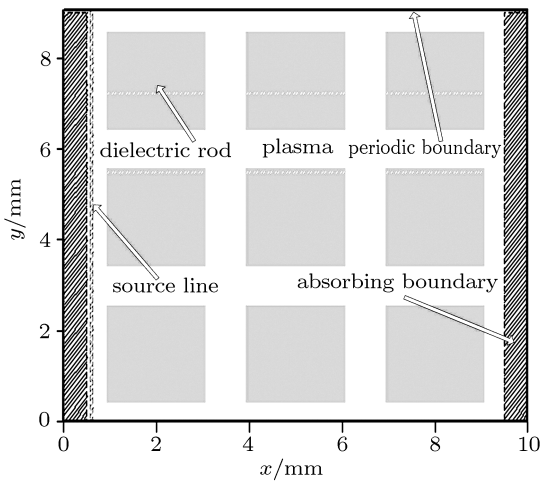


Fig. 5. The DPPC geometry used in PIC simulation.

[1)] CHIPIC Studio 3.2, Version 1.0 June 2006.

Figure 6(a) shows the input spectrum of electric field E_z which is a Gaussian distribution with frequency spans from 0 GHz to 120 GHz. Note that the propagation of wave is along the x direction which is corresponding to the $\Gamma - X$ direction in DPPC. Figure 6(b) shows the output spectrum, compared with the input spectrum, there is a series of pass and stop band below plasma frequency $\omega_{\rm p} = 2\pi \times 100$ GHz while wave cannot propagate in bulk plasma. The transmission characteristic of DPPC shows a potential use in PC filter which can be modified in width and position by varying period or plasma frequency.

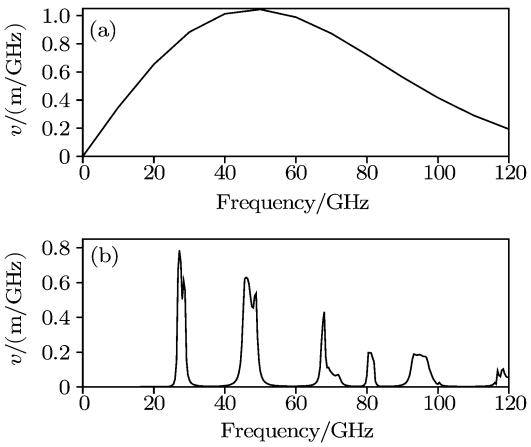


Fig. 6. (a) Input spectrum of source line and (b) output spectrum of detector line in DPPC.

Figure 7 shows the dispersion curves together with the transmission curve in DPPC. The left side is the unidirectional dispersion curves in the $\Gamma - X$ direction, while the right side is transmission curve obtained by division between the outputted and inputted spectrum in Fig. 6. The transmission and the dispersion curves have the same vertical axis which denotes the normalized frequency. The bottom horizontal axis of dispersion curves means wave vector $\boldsymbol{k}$ in the $\Gamma - X$ direction, and the top horizontal axis of the transmission curve indicates normalized magnitude. In Table 1, band gaps whose the normalized magnitude of transmission curve is less than 0.1 are compared with those of the dispersion curves in the $\Gamma - X$ direction, and they are basically in agreement with each other.

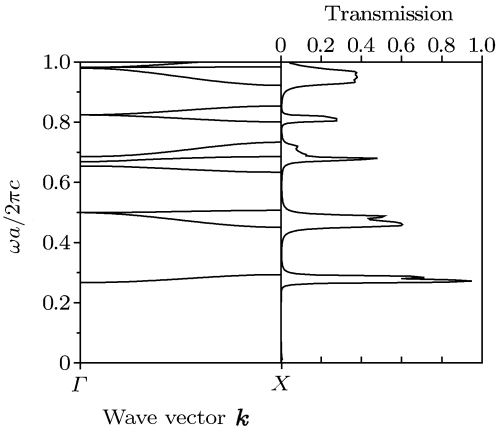


Fig. 7. Dispersion curves (left side) and transmission curve (right side) of TM mode in the $\Gamma - X$ direction.

Table 1. Comparison of band gap between dispersion curves and transmission curve of TM mode in the $\Gamma - X$ direction.

band gap (dispersion curves)	band gap (transmission curve)
0.00–0.270	0.00–0.264
0.294–0.451	0.296–0.445
0.500–0.634	0.502–0.660
0.733–0.801	0.720–0.800
0.854–0.922	0.828–0.924

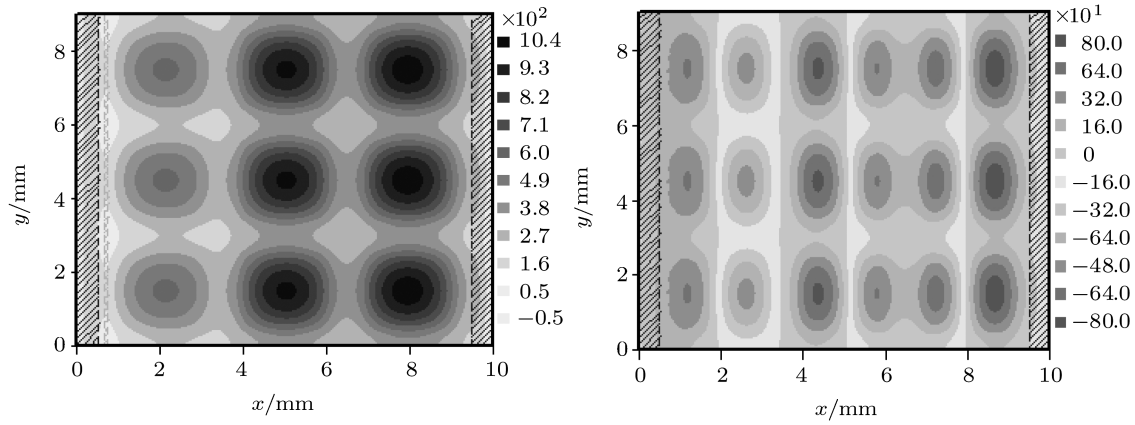


Fig. 8. Contour plots of E_z (a) at $t = 0.55$ ns for $f = 27$ GHz and (b) at $t = 1.95$ ns for $f = 47$ GHz by PIC simulation.

Using the method of PIC simulation, we can clearly observe the propagating process of any monochromatic signal at distinct time and space through the contour plots of field. Figure 8(a) shows the contour plot of E_z at 0.55 ns for the first mode at 27 GHz, and Fig. 8(b) shows the contour plot of E_z at 1.95 ns for the second mode at 47 GHz. For the first mode at 27 GHz, the electric field is strongly concentrated in the high-dielectric regions, while for the second mode at 47 GHz, a nodal plane cuts through the high-dielectric rods, expelling some of the electric field to the plasma region. The contrast between the two modes can explain a large gap between them as that of solid dielectric PC.[25,26]

4. Conclusions

In conclusion, using modified PWM, we examine dispersion characteristics of the TM mode for 2D DPPC. It is seen that the wave can propagate below plasma frequency in DPPC and this can be explained by the Maxwell–Garnett effective medium theory. The EPF decreases exponentially as the dielectric filling factor increases for a given dielectric, and for a given filling factor, EPF decreases with the increase of the dielectric constant of dielectric rod. It is also found that there are large omnidirectional band gaps in DPPC due to the weak coupling between dielectric rods, band gaps enlarge with the increase of plasma frequency. To study the process of the electromagnetic field as a function of time and space in DPPC, PIC simulation is carried out and the transmission curve in PIC simulation is consistent with the dispersion curves calculated by modified PWM. By comparing the electric field patterns at the transmission points of 27 GHz and 47 GHz in PIC simulation, the large gap between them can be qualitatively explained.

References

[1] Yablonovitch E 1987 *Phys. Rev. Lett.* **58** 2059
[2] John S 1987 *Phys. Rev. Lett.* **58** 2486
[3] Hojo H and Mase A 2004 *J. Plasma Fusion Res.* **80** 89
[4] Liu S, Hong W and Yan N 2006 *Int. J. Inf. and MmW.* **27** 403
[5] Ma L, Zhang H F and Liu S B 2008 *Acta Phys. Sin.* **57** 5089 (in Chinese)
[6] Zhang H F, Ma L and Liu S B 2009 *Acta Phys. Sin.* **58** 1071 (in Chinese)
[7] Sakai O, Sakaguchi T and Tachibana K 2007 *Contrib. Plasma Phys.* **47** 96
[8] Sakai O, Sakaguchi T and Tachibana K 2005 *Appl. Phys. Lett.* **87** 241505
[9] Sakai O, Sakaguchi T and Tachibana K 2007 *J. Appl. Phys.* **101** 073304
[10] Sakai O, Sakaguchi T and Tachibana K 2007 *J. Appl. Phys.* **101** 073305
[11] Sakai O and Tachibana K 2007 *IEEE Trans. Plas. Sci.* **35** 1267
[12] Meade R D, Rappe A M, Brommer K M, Joannopoulos J D and Alerhand O L 1993 *Phys. Rev.* B **48** 8434
[13] Kuzmiak V, Maradudin A A and Pincemin F 1994 *Phys. Rev.* E **50** 16835
[14] Wang R, Wang X H, Gu B Y and Yang G Z 2001 *J. Appl. Phys.* **90** 4307
[15] Luebbers R J, Hunsberger F and Kunz K S 1991 *IEEE Trans. Antennas Propagat.* **39** 29
[16] Pendry J B and MacKinnon A 1992 *Phys. Rev. Lett.* **69** 2772
[17] Li L M and Zhang Z Q 1998 *Phys. Rev.* B **58** 9587
[18] Zhang W, Chan C T and Sheng P 2001 *Opt. Express* **8** 203
[19] Xu X C, Xi Y G, Han D Z, Liu X H and Zi J 2005 *Appl. Phys. Lett.* **86** 091112-1
[20] Pendry J B, Holden A J, Stewart W J and Youngs I 1996 *Phys. Rev. Lett.* **76** 4773
[21] Granqvist C G and Hunderi O 1977 *Phys. Rev.* B **16** 3513
[22] Weissker H C, Furthmuller J and Bechstedt F 2003 *Phys. Rev.* B **67** 165322
[23] Fan C Z, Wang G and Hang J P 2008 *J. Appl. Phys.* **103** 094107
[24] Sakurai J J 1994 *Modern Quantum Mechanics* (New York: Addison-Wesley)
[25] Meade R D, Rappe A M, Brommer K D and Joannopoulos J D 1993 *J. Opt. Soc. Am.* B **10** 328
[26] Joannopoulos J D, Johnson S G, Winn J N and Meade R D 2008 *Photonic Crystals-Molding the Flow of Light* (Princeton: Princeton University Press) p69